Quantification of Solution-Free Blood Cell Staining by Sorption Kinetics of Romanowsky Stains to Agarose Gels

Chae Yun Bae[1,$,#], Hamid Esmaeili[2,$], Syed A. Zamin[2], Min Jeong Seol[1], Eunmi Hwang[1], Suk Kyung Beak[1], Younghoon Song[1], Bhuvnesh Bharti[3], Jangwook P. Jung[2,#]

1. Noul Co., Ltd. Yongin-si, Gyeonggi-do, Republic of Korea
2. Department of Biological Engineering, Louisiana State University, Baton Rouge, LA, U.S.A.
3. Cain Department of Chemical Engineering, Louisiana State University, Baton Rouge, LA, U.S.A.

[$]These authors contributed equally.
[#]Co-corresponding authors

Corresponding authors[#]

Jangwook P. Jung, PhD
Department of Biological Engineering
Louisiana State University
Baton Rouge, LA 70803, U.S.A.
Phone: +1-225-578-2919
Fax: +1-225-578-3492
E-mail: jjung1@lsu.edu

Chae Yun Bae, PhD
Noul Co., Ltd.
Yongin-si, Gyeonggi-do
Republic of Korea
Postcode: 16942
Phone: +82-70-4352-5861
Fax: +82-31-893-6671
E-mail: christina@noul.kr

Abstract

Imaging and quantification of stained blood cells are important for identifying the cells in hematology and for diagnosing diseased cells or parasites in cytopathology. Romanowsky staining have been used traditionally to produce hues in blood cells using anionic eosin Y and cationic methylene blue. While Romanowsky stains have been widely used in cytopathology, end-users have experienced problems with varying results in staining due to premature precipitation or evaporation of methanol, leading to the inherent inconsistency of solution-based Romanowsky staining. Here, we demonstrate that staining and destaining of blood smear are controllable by the contact time of agarose gel stamps. While the extent of staining and destaining are discernable by hue values of stamped red blood cells in micrographs, quantification of adsorbed and desorbed Romanowsky dye molecules (in particular, eosin Y, methylene blue, and azure B) from and to the agarose gel stamps needs a model that can explain the sorption process. We find predictable sorption of the Romanowsky dye molecules from the pseudo-second-order kinetics models for adsorption and the one phase decay model for desorption. Thus, the method of agarose gel stamping demonstrated here could be an alternative to solution-based Romanowsky staining with predictable quantity of sorption and timing of contact.

Keywords

Solution-free staining, Romanowsky stain, adsorption, desorption, miLab

Introduction

Hydrogels are polymeric networks capable of integrating large amount of water within their molecular structure. The application of hydrogel technology in biomedicine includes drug delivery, surgical tools, cosmetics, device coatings, and tissue regeneration to name a few [1]. In an effort to perform blood or pathology tests without accessing to a large clinical center [2, 3], we utilized agarose to fabricate hydrogel stamps to leverage solution-free stamping technology to detect white blood cells (WBCs) and malaria-infected red blood cells (RBCs) [4]. Upon solidification, agarose forms nanometer-scale pores ranging from 100 to 200 nm [5], which is advantageous for adsorption and desorption of Romanowsky dyes. Since the gelation of agarose is predominantly driven by hydrogen bonds and electrostatic interactions, packaging Romanowsky dyes in agarose gels requires no further modification of the agarose gels or Romanowsky dyes to apply this stamping technology. Agarose exhibits a high rate of dye removal over multiple adsorption-desorption cycles in comparison to gelatin [6], alginate [7] and polyaniline [8] composites. Agarose gels do not exhibit swelling or shrinkage in aqueous buffer [9], which allows fabrication of hydrogel stamps with high precision and maintains excellent mechanical properties. While the application of the hydrogel stamping method demonstrates that the solution-free staining is a better alternative to several solution staining methods, quantitative characterization of sorption kinetics on the hydrogel stamping with the ternary mixture of Romanowsky stains is yet to be achieved.

As shown in **Figure 1**, we demonstrate that staining and destaining of smeared RBCs using the agarose hydrogel stamps with the ternary mixture of Romanowsky dyes are quantifiable by evaluating hue values of micrographs. For quantitative assessment of adsorbed or desorbed amount of Romanowsky dyes, we performed adsorption and desorption of the ternary mixture of Romanowsky dyes to and from agarose gels. We found that isotherms and different kinetics models can be employed to estimate the quantity of Romanowsky dyes for the solution-free hydrogel stamping technology.

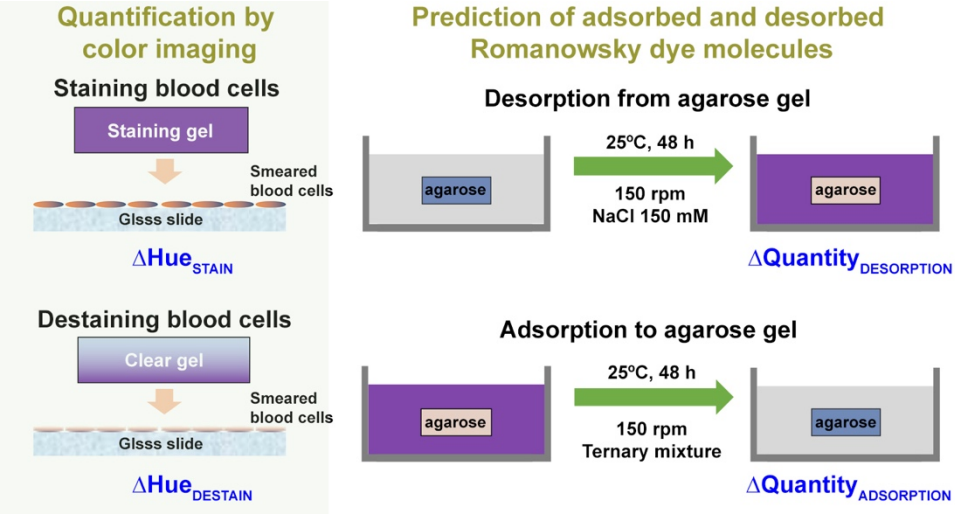

Figure 1. Overall schematic of the experiments for quantification. First, we stained and destained RBCs with the agarose hydrogel stamps and the values of hue (H) were assessed with respect to contact time. For quantitative assessment, we measured concentration changes and employed isotherms and kinetics models.

Materials and Methods

We purchased eosin Y disodium salt (EY, cat# E4382-25G, Sigma-Aldrich), methylene blue (MB, cat# M9140-25G, Sigma-Aldrich), azure B (AZB, cat# A4043-5G, Sigma-Aldrich), agarose (Agarose, cat# A4679, Sigma-Aldrich), methanol (cat# 179957, Sigma-Aldrich) and used without any further modification. The collection and application of whole blood were approved by the Institutional Review Board (P01-202003-31-007) of the Korea National Institute for Bioethics Policy (Seoul, Korea).

Formation of ternary mixture stamps to quantify staining and destaining of RBCs

To prepare the blood film, 4 μL of whole blood was dropped on the precleaned glass slide and smeared in the miLab™ (Noul Co., Ltd.). Then, the smeared glass (smear width, 1.6 cm) was fixed for 2 min in methanol. To stain and destain blood cells, 0.7 mL of circular agarose gel (2% w/v, diameter of 2 cm and height of 0.22 cm) was created and submerged to the ternary mixture solution (EY 3.5 μM; MB 70 μM; AZB 140 μM). The circular agarose gel

was incubated on the rocker with 150 rpm at room temperature for 48 h. Before and after the incubation of the agarose gel, absorbance of ternary mixture was measured at 518, 645 and 664 nm. After 48 h of incubation for adsorption, all the agarose gel were collected and applied to the blood smeared slides for staining. The circular agarose gel was put on the smeared blood films and incubated for 10 s, 30 s, 60 s and 600 s for staining. At the end of staining, the circular agarose gel was removed and stained blood smeared slides were dried for 10 s. Then, the circular agarose gel without any Romanowsky dyes was placed on the stained region of the slide to destain the smeared blood cells. The destaining time was also varied from 10 s, 30 s, 60 s and 600 s. After destaining of smeared blood cells, slides were dried for 10 s.

Application of miLab™ hydrogel stamps to blood films

To prepare the blood film, 5 μL of whole blood was dropped on the precleaned glass of the miLab™ cartridge, which was inserted into the miLab™ (Noul Co., Ltd.). Each miLab™ cartridge consists of red, blue and clear agarose gels. The red agarose gel contains EY, the blue agarose gel contains MB and AZB and the clear agarose gel contains no Romanowsky stains [4]. For simulated conditions, we stained the blood film with the red agarose gel for 10 s, the blue agarose gels for 60 s and the clear agarose gels for 30 s sequentially. To compare the extent of staining with different combinations of red, blue and clear agarose gels, the blood films were stained and destained with different combinations of 10 s, 30 s and 60 s.

Imaging of stained blood cells after stamping with agarose gels

At least three images from three different slides were acquired using a microscope (Olympus CX33, 50× NA: 0.50 or 100× NA: 0.95, exposure 200 ms). In each image, 50 RBCs were randomly selected. In each RBC, the region of interest (ROI) was defined as a diameter of 7 μm. Then, the RGB values at the ROI were extracted from the split images with red, green

and blue channels using Image J. Then, mean values (0-255) of red (R), green (G) and blue (B) were normalized by dividing 255 (R', G' and B', respectively) and transformed to HSV (hue, saturation and value) values with the following equation [10]:

$$\Delta = C_{max} - C_{min};\ C_{max} = \max(R', G', B') \text{ and } C_{min} = \min(R', G', B') \quad \textbf{(1)}$$

$$H = 60° \times [(G' - B') \times \mathrm{mod}6/\Delta],\ C_{max} = R',\ \mathrm{mod}6 = \text{remainder after dividing by } 6 \quad \textbf{(2-1)}$$

$$H = 60° \times [(B' - R')/\Delta + 2],\ C_{max} = G' \quad \textbf{(2-2)}$$

$$H = 60° \times [(R' - G')/\Delta + 4],\ C_{max} = B' \quad \textbf{(2-3)}$$

$$H = 0° \text{ when } \Delta = 0$$

$$S = \Delta/(1 - |2L-1|),\ \Delta \neq 0;\ S = 0,\ \Delta = 0 \quad \textbf{(3)}$$

$$V = C_{max} \quad \textbf{(4)}$$

Oscillating rheometry

Samples for oscillating rheometry were cast using custom molds of 8 mm diameter and 2 mm height. Agarose gels at 20 mg/mL including different combinations of dyes, types of buffer (HEPES 50 mM) or additives (Tween-20 0.5% (w/v)) were prepared. For comparison, the ternary mixture was adsorbed for 48 h at 150 rpm. Both storage (G′) and loss (G″) moduli of agarose gels were determined by frequency sweeping from 0.628 to 62.8 (rad/s) at a strain of 10% using a TA Discovery HR-2 rheometer with an 8-mm parallel plate.

Calculation of concentrations of ternary mixtures

To decide a peak wavelength of each Romanowsky dye, samples were transferred into 96-well plates for absorbance measurement using a Cytation3 Spectrophotometer and

absorbance were plotted against wavelengths ranging from 450 to 700 nm (**Figure S1**). The peak wavelengths of each dye were decided at 518, 664 and 645 nm for EY, MB [11] and AZB [12], respectively. By observing the absorbance values of the unknown at each peak wavelength correlated with the peak of individual Romanowsky dye, we were able to solve the system of equations:

$$A_1 = \varepsilon^1_{EY} C_{EY} \ell + \varepsilon^1_{MB} C_{MB} \ell + \varepsilon^1_{AZB} C_{AZB} \ell \,(\text{at } \lambda_1) \quad \textbf{(5)}$$

$$A_2 = \varepsilon^2_{EY} C_{EY} \ell + \varepsilon^2_{MB} C_{MB} \ell + \varepsilon^2_{AZB} C_{AZB} \ell \,(\text{at } \lambda_2) \quad \textbf{(6)}$$

$$A_3 = \varepsilon^3_{EY} C_{EY} \ell + \varepsilon^3_{MB} C_{MB} \ell + \varepsilon^3_{AZB} C_{AZB} \ell \,(\text{at } \lambda_3) \quad \textbf{(7)}$$

for C_{EY}, C_{MB}, and C_{AZB}, the concentrations of EY, MB, and AZB, where ε^X_{EY}, ε^X_{MB} and ε^X_{AZB} represent the coefficient of extinction for EY, MB and AZB at a specific wavelength *X*. A_X represents the absorbance value at wavelength *X*, ℓ is the path length and λ_1, λ_2, λ_3 correlate with peaks of the individual dyes' absorption spectra.

Adsorption isotherms of ternary mixtures to agarose gels

The agarose precursor solution was transferred to a custom-made hollow cylinder using 1 mL syringe (cat#309628, BD) and allowed to solidify. To assess the adsorption capacity of the agarose gels, a total of 3.5 mL ternary mixture and agarose gels (20 mg/mL) in a 50 mL tube were added. Thiazine molecules can be adsorbed to glass, thus we performed all adsorption and desorption experiments with polypropylene plasticware [13]. The tubes were shaken (150 rpm) at room temperature for 48 h. Concentrations were measured and calculated at the end of 48 h. The initial and final absorbances of each Romanowsky dye were measured by a Cytation3 spectrophotometer or a VersaMax (Molecular Devices, CA) and the concentrations were calculated by the system of equations **(5)** through **(7)**. The adsorption capacity (q_e, mg/g) was calculated using the following equation:

$$q_e = [(C_0 - C_e)V]/m \quad \textbf{(8)}$$

where C_0 and C_e are the initial and final concentrations of each Romanowsky dye in the ternary solution, respectively, V is the volume of the ternary solution (3.5 mL), and m is the dry weight of adsorbent (14 mg).

The Langmuir model assumes monolayer coverage of dyes over a homogeneous sorbent surface [14]. Thus, the Langmuir adsorption isotherm is a commonly used isotherm model describing the adsorbate-adsorbent interactions by the following equation:

$$q_e = (Q_{sat}K_LC_e)/(1+K_LC_e) \quad \textbf{(9)}$$

where C_e (mg/L) is the equilibrium concentration in solution; q_e (mg/g) is the adsorption capacity at equilibrium; Q_{sat} (mg/g) is the maximum adsorption capacity; K_L (L/mg) is the Langmuir adsorption equilibrium constants.

Kinetics of adsorption and desorption of ternary mixtures to agarose gels

To assess the kinetics of adsorption, the agarose gels were prepared with the same manner to construct isotherms. For adsorption kinetics, 165 µL of samples (EY 3.5 µM; MB 70 µM; AZB 140 µM) were moved to a well in 96-well plate and absorbance at 518 nm, 645 nm and 664 nm were measured at different time points (0.33, 0.66, 1, 1.33, 1.66, 2, 4, 6, 24, and 48 h). Immediately after 48 h of adsorption, agarose gels were moved to fresh 3.5 mL of 150 mM NaCl solution in new 50 mL conical tubes. Conical tubes containing these gels were shaken at 150 rpm at room temperature for another 48 h. The method of concentration measurement and time points were the same for isotherms. The three models were used to fit the data. The pseudo-first order (PFO) kinetics model was plotted as following:

$$q_t = Q_e\,(1 - \exp[-k_1t/2.303]) \quad \textbf{(10)}$$

where q_t (mg/g) is the amount adsorbed/desorbed at time t (min), Q_e (mg/g) is the equilibrium adsorption capacity, and k_1 is the adsorption rate constant (L/min). The pseudo-second order (PSO) kinetics model was plotted as following:

$$q_t = Q_e^2k_2t/[1+Q_ek_2t] \quad (\textbf{11})$$

where q_t (mg/g) is the amount adsorbed at time t (min), Q_e (mg/g) is the equilibrium adsorption capacity, and k_2 is the adsorption rate constant (g/mg min^{-1}). The intraparticle diffusion (IPD) model was applied as following:

$$q_t = k_3 t^{1/2} + C \quad \textbf{(12)}$$

where q_t (mg/g) is the amount adsorbed at time t (min), k_3 is the adsorption rate constant (g/mg $min^{-1/2}$) and C is a constant associated with the boundary layer effect. To assess the kinetics of desorption, data were fitted with the one phase decay model:

$$q_t = (Q_{max} - Q_{min}) \exp(-t/\tau) + Q_{min} \quad \textbf{(13)}$$

where Q_{max} or Q_{min} (mg/g) is the maximally or minimally adsorbed quantity at time t (min), respectively, and τ is the characteristic decay time (min).

Statistical analysis

For quantification of H or S, 198 RBCs were counted for staining/destaining data and 40 ROIs were counted for background data, with three different smeared slides. The statistical significance between sample and control was calculated by one-way ANOVA with Dunnett's multiple comparison or with Tukey's *post hoc* test (α=0.05) where $p < 0.05$ was considered statistically significant.

Results and Discussion

The extent of staining and destaining to and from RBCs is quantifiable by values of hue.

To assess the required time for RBC staining by the ternary mixture adsorbed agarose gels, we used hue (H) from micrographs. While the RGB color space can produce a wide variety of colors, the relationship between the constituent amounts of red (R), green (G) and blue (B) light and the resulting color is not intuitive [15]. H is what we most often think as color and is represented by a single number in 360 degrees: red is 0, yellow is 60, green is 120 and cobalt is

240. The HSV (hue, saturation, value) color space has been widely applied in cytopathology since this approach is designed to align more closely with the way human vision perceives color attributes. Examples include the analysis of whole blood components [10, 16], histological images with reduced variation [17] or colon tissue images to detect cancers using convolutional neural network (CNN) [18]. In Romanowsky staining, the dyes containing acidic EY (red) and basic AZB (oxidized MB, blue-purple) produce neutral stains, where basic AZB binds to the anionic (acidic) nuclei and acidic EY binds to highly cationic (basic) cytoplasm. MB that has undergone oxidative demethylation is knowns as polychrome MB, which has about 11 dyes including azure A, azure B, azure C, methylene blue, methylene violet Bernthesen, methyl thionoline, and thionoline [19]. The Romanowsky effect describes the production of purple color in the chromatins of the nucleus and the certain granules in the cytoplasm of blood cells when AZB combines with EY to give azure B-eosin complexes [20]. In principle, Romanowsky staining works to produce a variety of H by modulating the ratios of MB/AZB to EY, solvent composition (methanol content), pH of phosphate buffer and timing of staining [20].

As shown in **Figure 1**, staining is the desorption of the ternary mixture dyes to RBCs and destaining is the adsorption of the ternary mixture dyes to agarose gels. First, we assessed the background H after staining the blood smear for 10 s, 30 s and 60 s with the ternary mixture adsorbed agarose gels. As shown in **Figure S2a**, background H from mostly plasma is around 200 (cerulean to azure) without strong time-dependency. However, the background H from RBC are around 80 (chartreuse to lime) for 10 s and around 100 (kelly green) for 30 s and 60 s (**Figure S2b**). As shown in **Figure S2b**, as the contact time increases, H from RBCs increases accordingly. However, the difference between 30 s and 60 s staining is statistically not significant ($p=0.977$ with Tukey's *post hoc* analysis). Moreover, the mean of H from RBC is decreased to around 70 (chartreus) in the case of 600 s staining. Next, we evaluated H with different staining-destaining durations, In **Figure 2a**, these H are collected after staining for 10 s and different destaining duration, as indicated in each column. We also plotted the background

H with the dotted line (RBC background). As expected, the longer destaining lasts, the more H decrease. In the given time frame up to 60 s, none of destaining completely removed the staining of RBCs as indicated that all mean H are higher than the RBC background line. In all cases of 60 s destaining, H increase (**Figure 2a** or **2c**) or remains somewhat similar to 30 s destaining (**Figure 2b**), which is indicative of possible resorption of dyes to RBCs from agarose gels after 30 s of destaining [4]. Destaining for 10 s after 60 s of staining (**Figure 2c**) is not enough to remove adsorbed Romanowski dyes from RBCs. In **Figure 2d**, H remains similar regardless of destaining duration, which makes difficult to infer the amount of transfer in the cycle of staining and destaining of RBCs. Due to the difficulties in the quantification, we decided not to assess the changes of H beyond 60 s.

H is the color sensed due to the wavelength and saturation (S) indicates the purity of the color. From equation (**4**), Value (V) does not appear to change with coloration quality. After we extracted S with respect to different periods of staining and destaining, we found that S is minimally changed (**Figure S3**) out of the entire range from 0 to 1. Thus, it is expected that S is not a good determinant to assess the extent of RBC staining from agarose gels with the ternary mixture. In contrast, H shown in **Figures 2** and **S2** ranges from 0 to above 200 and shows relatively wider and distinguishable ranges. Thus, the feature of our analysis is determined with values of H in the HSV color space.

As shown in **Figure 3a**, staining of RBCs with the ternary mixture adsorbed agarose gel increases values of H monotonically up to 30 s. Values of H in 10 s and 30 s destaining also monotonically decrease while those of 60 s decrease a bit irregular with more pronounced changes between 10 s and 30 s of destaining otherwise with relatively small changes (**Figure 3b**). During 60 s of staining, values of H increase up to 100 (lime to kelly green) because of the desorption of MB or AZB from agarose gels. If the contact time increases up to 600 s, however, values of H decrease to around 70 (chartreuse) because the cytoplasm of RBC is predominantly stained by EY. Data presented in **Figures 2** and **3** demonstrate that the extent of staining and

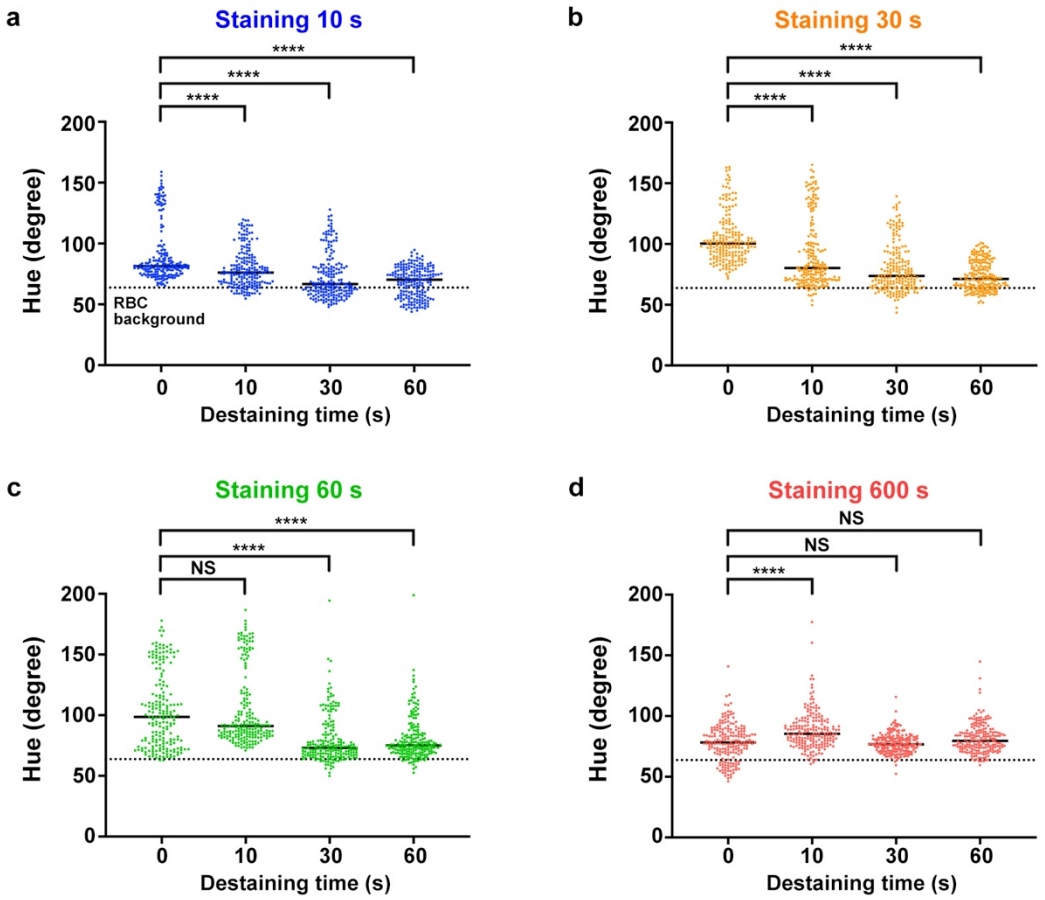

Figure 2. Changes in values of H with respect to different periods of staining and destaining of RBCs. In (a-d), destaining was performed for 10 s, 30 s and 60 s after 10 s (a), 30 s (b), 60 s (c) and 600 s (d) of staining. N=3 samples and 120 blood cells in each column, One way ANOVA with Dunnett's multiple comparison tests, ****p<0.0001 and NS (non-significant). Scatter dot plot with mean.

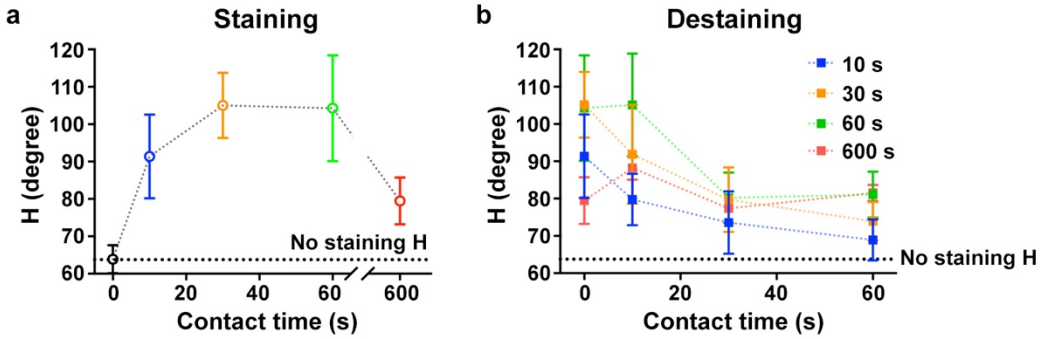

Figure 3. Changes in values of H during staining and destaining of RBCs. (a) Staining of RBCs is tracked at 10 s, 30 s, 60 s and 600 s. (b) Destaining of RBCs is tracked in three different periods of staining 10 s (blue), 30 s (orange), 60 s (green) and 600 s (red). Mean±SEM, 120 data points and n=3 samples.

destaining to RBCs are quantifiable. In addition, we are able to discern colorfulness by values of H. To quantify the amount of Romanowsky dye transfer, it is imperative to directly measure the concentration changes in the cycle of staining and destaining. Next, we adsorbed the ternary mixture to agarose gels and desorbed the adsorbed ternary mixture from the agarose gels to buffer solution to determine isotherms and kinetics models of the Romanowski dye transfer.

Concentrations of ternary mixtures are calculable by the system of equations.

To determine the concentrations of ternary mixtures, we used an approach with systems of equations [21, 22] to calculate the concentrations of each Romanowski dye in a solution containing a mixture of EY, MB and AZB. We found that those intercepts are close to zero and those R^2 values of each curve are 0.99 (**Figure 4**). This allows us to set up the following system of equations:

$$A_1 = 40.5\ C_{EY} + 1.37\ C_{MB} + 1.77\ C_{AZB} \quad \textbf{(5-1)}$$

$$A_2 = 0.0120\ C_{EY} + 21.0\ C_{MB} + 22.8\ C_{AZB} \quad \textbf{(6-1)}$$

$$A_3 = 0.0163\ C_{EY} + 26.8\ C_{MB} + 13.9\ C_{AZB} \quad \textbf{(7-1)}$$

Some coefficients are lower than others. For example, coefficients of C_{MB} or C_{AZB} are smaller than that of C_{EY} in equation (**5-1**), indicating that A_1 values are predominantly determined by C_{EY} since the concentration change of EY is more apparent at the wavelength of 518 nm than those at 645 or 664 nm (**Figure 4a**). However, in equations (**6-1**) and (**7-1**), coefficients of C_{MB} or C_{AZB} are somewhat similar to each other, meaning that MB and AZB dyes are expected to have similar absorbance (**Figures 4b** and **4c**). In addition, none of the coefficients in equations (**5-1**) to (**7-1**) are zero, it is imperative to use all of coefficients (3×3 matrix coefficients in **(14)**) to calculate the concentrations of any ternary mixture in our study.

$$\begin{bmatrix} A_1 \\ A_2 \\ A_3 \end{bmatrix} = \begin{bmatrix} 40.5 & 1.37 & 1.77 \\ 0.0120 & 21.0 & 22.8 \\ 0.0163 & 26.8 & 13.9 \end{bmatrix} \begin{bmatrix} C_{EY} \\ C_{MB} \\ C_{AZB} \end{bmatrix} \quad (\textbf{14})$$

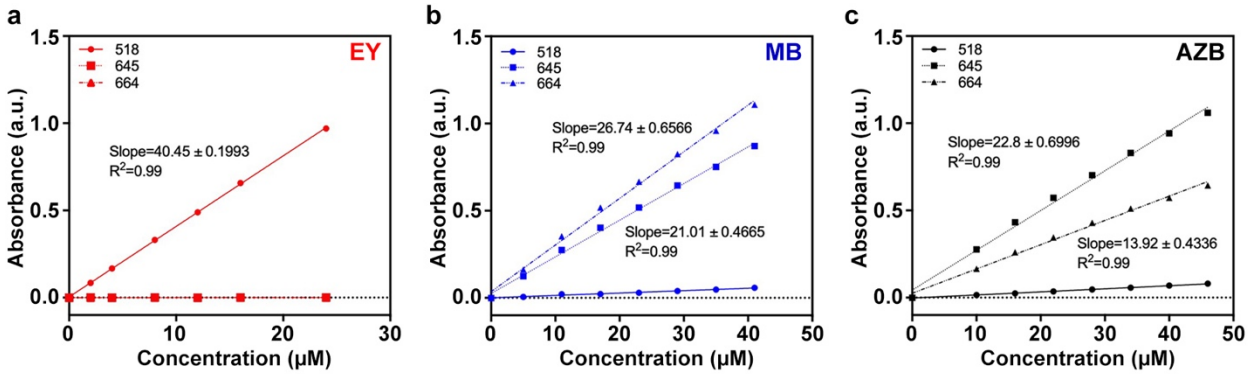

Figure 4. Standard curves to evaluate concentrations of the ternary mixture. To calculate concentrations of ternary mixtures of EY (a), MB (b) and AZB (c) at three different wavelengths (518 nm, 664 nm, and 645 nm, respectively), the linear regression formula and R^2 (all >0.99) are denoted. The slope of each regression equations from **5-1**, **6-1** and **7-1** are used for the coefficient matrix (**14**); n=3, mean±SD.

Shear modulus of agarose gels is maintained when Romanowski dyes are adsorbed after the solidification of agarose gels.

In our previous publication [4], we demonstrated that the hydrogel stamping technology is a simple, reproducible, solution-free, and inexpensive approach to stain blood cells. The delivery and removal of dyes are mediated by agarose gels. The microstructure of agarose gels consists of a dense interwoven network of fibers and pores [5, 9, 23] ranging from 100 – 200 nm [24]. A single molecule of MB has a cross-section of 0.8-0.9 nm [25, 26], and thus can pass freely through pores of agarose gels. AZB is the oxidized form of MB and has similar topological polar surface areas (TPSA) to that of MB (MB, 0.439 nm^2 and AZB, 0.527 nm^2). Therefore, it is reasonable to assume that the molecular cross-section of AZB would be similar to 0.8-0.9 nm and thus physical interaction of MB and AZB within the pores of agarose gels would be similar. In contrast, the diameter of EY is around 1.6 nm (TPSA of EY, 0.838 nm^2) [27], thus we expect to see different extent of interactions of EY with agarose gels.

Initially, we hypothesized that the bulk mechanical properties of agarose gels are altered upon mixing with Romanowski dyes during solidification or upon adsorption after the solidification of agarose gels. We found that mechanical properties of agarose gels were altered upon the addition of individual or mixture of Romanowski dyes during solidification. Dyed

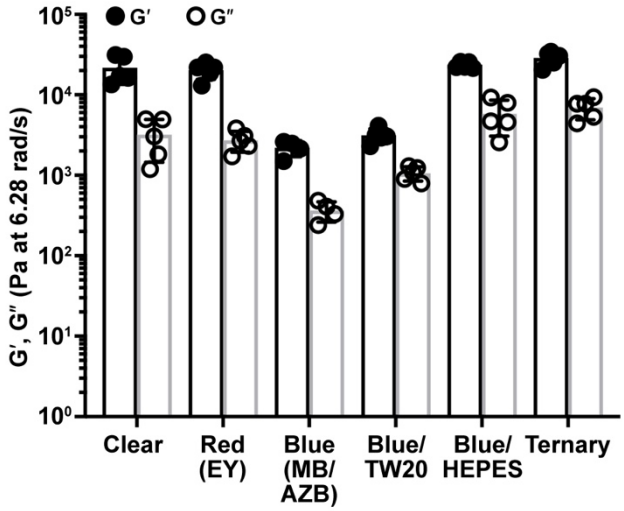

Figure 5. Viscoelasticity of agarose gels with Romanowski dyes mixed during solidification or adsorbed after solidification. Viscoelasticity of clear, red (EY) and blue (MB/AZB) agarose gels as well as the ternary mixture adsorbed agarose gel is compared at 6.3 rad/s (1 Hz). Storage (G′) and loss (G″) modulus, mean±SD, n=5.

agarose gels were prepared by mixing EY or MB:AZB (1:2 ratio) before solidification of agarose gels [4]. While the red and the clear agarose gels maintained storage modulus around 20 kPa and loss modulus around 3 kPa, the addition of MB and AZB before solidification significantly altered both storage and loss moduli, as evidenced in **Figure 5**. In contrast, after adsorbing the ternary mixture to agarose gels for 48 h, we did not find any significant difference of shear modulus (both storage and loss moduli) between the ternary mixture adsorbed agarose gel and either the blue agarose gel with HEPES or the clear agarose gels (**Figure 5**). Upon cooling of agarose solution, the polysaccharide chains of agarose made of the repeating unit of *D*-galactose and 3,6-anhydro-*L*-galactopyranose are aligned and form a mesh of channels of diameter from 100 – 200 nm, where the structure is held together by hydrogen bonding. To restore mechanical properties of the blue agarose gels, we attempted to include an additive in the blue agarose gels. Nonionic surfactant polysorbate 20 (Tween-20) only increase loss modulus (G″) of the blue agarose gels to certain extent, not the storage modulus. However, 50 mM of HEPES (4-(2-hydroxyethyl)-1-piperazineethanesulfonic acid) increased both storage and loss moduli. HEPES is a zwitterionic molecule that can stabilizes polysaccharide-thiazine (an

organic compound containing a ring of four carbon, one nitrogen and one sulfur atom such as MB) dye by shielding electrostatic interactions [28]. It is reported that the adsorption of MB is primarily mediated by polysaccharides functional groups such as C–C, C–O and C–O–C [29, 30]. However, adsorption of ternary mixture to solidified agarose gels did not alter the mechanical properties. Since small molecules, i.e. dye or detergent, are presumably adsorbed to the surface or pores of agarose gels after solidification, the alignment or networking of polysaccharide chains are not likely interfered.

Isotherms of adsorption allow us to narrow down the concentration ranges of the ternary mixture for kinetics experiments.

To estimate the limit of adsorption of Romanowski dyes to agarose gels, we performed adsorption of ternary mixtures at multiple concentrations for 48 h. Adsorption isotherms of individual dye show that the Langmuir isotherm explains the adsorption of molecules of each Romanowski dye to agarose gel surface (**Figures 6a, 6b** and **6c**) with high goodness of fit (R^2=0.999). The Langmuir constant (K_L) of EY is 93.3 L/mg and those of MB and AZB are 33.3 L/mg and 21.1 L/mg, respectively (**Table 1**). This result supports that EY exhibits a stronger interaction with agarose gels than that of MB or AZB with agarose gels. The Langmuir model fits adsorption data well, indicating that the amount of adsorbed Romanowski dye molecules is saturated at higher concentrations.

From the molecular structures (EY is an anionic xanthene and MB or AZB is cationic thiazine) and size of each Romanowski dye molecule, we expect that the adsorption could be classified into two groups. As shown in **Table 1**, EY has stronger binding to the surface of agarose (higher K_L , binding strength of Romanowski dyes to the surface of agarose gels) than either MB or AZB does. This is possibly attributed to the larger TPSA of EY and/or preferential biding through the pores of agarose, while the adsorption of MB or AZB is likely non-specific and promiscuous throughout the surface or pores of agarose gels. Apparently, the absorbance

spectra of MB and AZB are not completely separated from each other (**Figure S1**), and **Figures 4b** and **4c** show such concurrent contribution to absorbance, which may have overestimation of Q_{sat}. Further, relatively lower concentration of EY in the ternary mixtures made the estimated Q_{sat} lower than those of MB or AZB. Collectively, it is expected that the amount of MB or AZB destaining from blood cells (removal of MB or AZB by agarose gels) would be larger than that of EY. Next, to further quantify the sorption of the ternary mixture over the course 48 h, we selected one of the higher concentrations tested in isotherms (EY 3.5 μM; MB 70 μM; AZB 140 μM) in assessing the kinetics. This concentration is higher enough to easily measure concentrations by UV-Vis and is closer to the asymptote in the sorption isotherms (**Figure 6a, 6b** and **6c**).

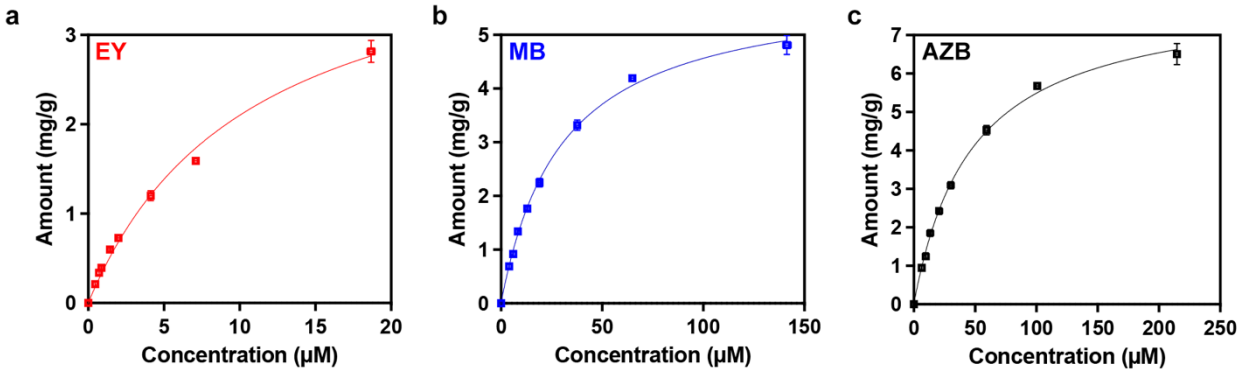

Figure 6. Adsorption isotherms of ternary mixtures. Isotherms of EY (a), MB (b) and AZB (c) are measured during the 48 h of adsorption; mean±SD, n=5.

Table 1. Parameters of the Langmuir isotherms.

Model	Parameters	Langmuir isotherm		
		EY	**MB**	**AZB**
Adsorption Isotherm	**Q_{sat} (mg/g)**	4.35	5.94	8.09
	K_L (L/mg)	93.3	33.3	21.1
	R^2	0.992	0.998	0.998

Adsorption and desorption kinetics show discernable affinities of Romanowski dye molecules to agarose gels.

To predict kinetics of adsorption and desorption, we measured concentration changes of

the selected ternary mixture during 48 h of adsorption and 48 h of desorption. As shown in **Figure 7**, the amount (mg/g) of dye adsorption and desorption approaches a maximum value asymptotically. While we fit three different kinetics models for adsorption (destaining, **Figure S4**), we find that the pseudo-second order (PSO) kinetic model fits with high R^2 values over the entire duration of 48 h (**Tables 2** and **S1**). The PSO kinetics model predicts that the adsorption rate is dependent on adsorption capacity, not on concentration of adsorbates [31], implying that a type of dye is a more important contributor than a concentration of dye in our hydrogel stamping technology. The pseudo-first order (PFO) kinetic model (**Figures S4**) also fits the adsorption of the ternary mixture over the entire duration of 48 h with relatively high R^2 values as well. The PFO kinetics model assumes that the rate of dye uptake is directly proportional to the difference between saturated concentration and the amount of dye uptake with time, which is generally applicable only over the initial stage of an adsorption process [31]. Therefore, the PSO kinetics model is presumably best fit in the range of 48 h for the kinetics of adsorption of the ternary mixture, indicating that the adsorption capacity of respective Romanowski dye molecules in agarose gels is the key determinant to understand the sorption kinetics. For all of our interpretation, we avoid the abuse of fitting kinetics data with the linearized models of kinetics and use nonlinear fitting methods with equations **(10)** through **(13)** [32].

After 48 h of adsorption, we assessed the quantity of Romanowski dye molecules in agarose gels over another 48 h (**Figures 7b, 7d** and **7f**) by fitting the desorption data with the one phase decay model [33]. As indicated by the filled areas, the binding affinity of EY is higher than both MB and AZB as evidenced by the ratio of Q_{min} to Q_{max} (**Table 3**). This result is also corroborated by higher values of K_L of EY than that of either MB or AZB (**Table 1**). These results show that around 50.0%, 75.5% and 81.9% of EY, MB and AZB, respectively, are released over the first 240 min (**Table S2**) and the rest of them is bound to agarose gels with high affinity (referred as the patterned areas in **Figures 7b, 7d** and **7f**).

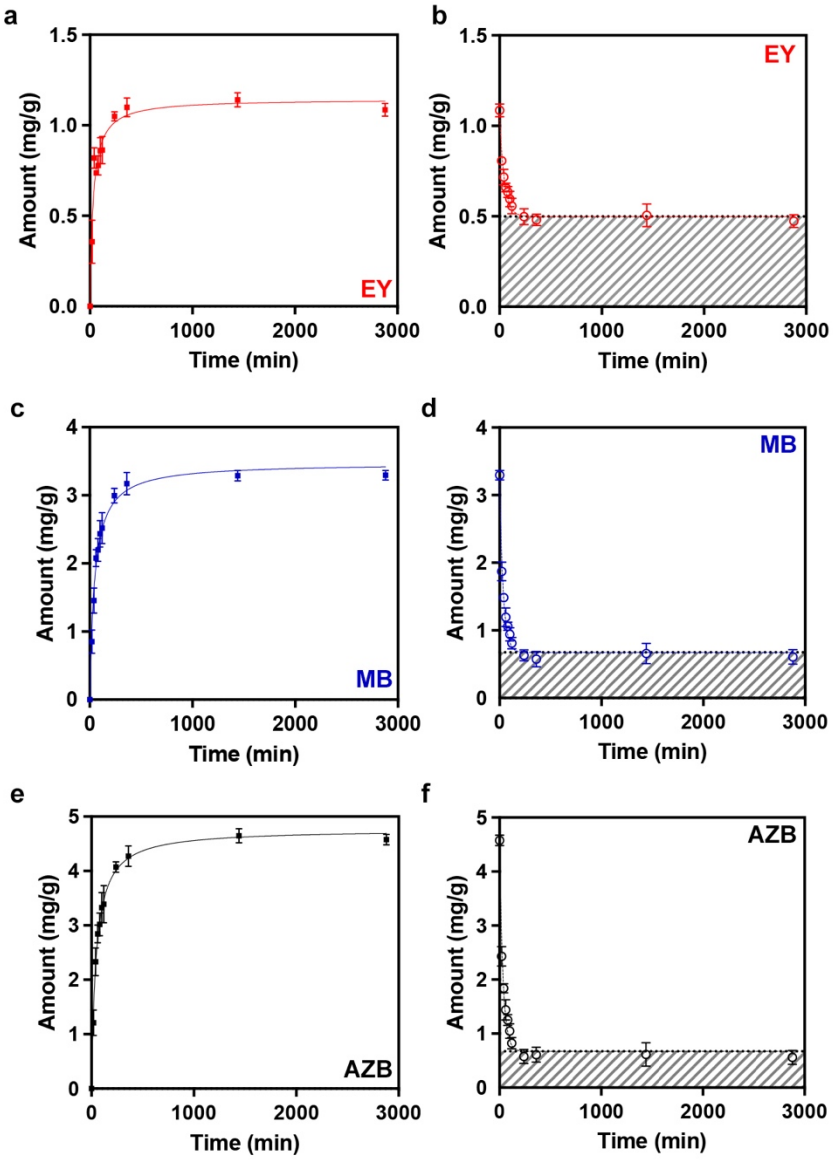

Figure 7. Adsorption and desorption kinetics of ternary mixtures. At a fixed concentration of the ternary mixture (EY 3.5 μM; MB 70 μM; AZB 140 μM), kinetics of adsorption (48h) of EY (a), MB (c) and AZB (e) is measured and fitted with the PSO kinetics models. The quantity of the ternary mixture of EY (b), MB (d) and AZB (f) retained in agarose gels was estimated by the one phase decay model. Patterned areas in (b), (d) and (f) indicate the quantity of each Romanowsky dye molecule with high affinity. mean±SD, n=5.

Table 2. Parameters of the PSO kinetics model (adsorption).

Model	Parameters	Adsorption		
		EY	**MB**	**AZB**
Pseudo-2nd-order kinetics (**PSO**)	**Q_e (mg/g)**	1.15	3.47	4.77
	k_2 (g/mg min^{-1})	0.0285	0.00612	0.00465
	R^2	0.959	0.990	0.994

Table 3. Parameters of the one phase decay kinetics model (desorption).

Model	Parameters	Desorption		
		EY	**MB**	**AZB**
One phase decay	**Q_{max} (mg/g)**	1.05	3.20	4.44
	Q_{min} (mg/g)	0.499	0.675	0.672
	τ (min)	47.3	35.2	34.3
	R^2	0.977	0.982	0.982

Further, considering the nature of the interactions between Romanowski dye molecules and agarose gels, the adsorption kinetics is possibly associated with the diffusion of Romanowski dye through the pores of agarose gels as discussed above. We fit the data with the intraparticle diffusion (IPD) of adsorbate (the Romanowski dye molecules) *via* two mechanisms: pore and surface diffusion [34]. In the IPD kinetics model, particle porosity (distribution and morphology) and tortuosity are key factors affecting the pore diffusion. As shown in **Figures S4** and R^2 values in **Table S1**, the IPD kinetics model showed low goodness of fit (values of R^2 being less than 0.6). If we fit the data with the IPD kinetics model up to 240 min, values of R^2 are higher (**Table S3**). Overall, the IPD kinetics model can explain the sorption kinetics better in earlier time points due to the pore diffusion of the Romanowski dye molecules. The larger EY molecules (diameter around 1.6 nm) showed relatively rapid adsorption probably bypassing the diffusion of smaller pores and the desorption is probably slowed due to steric hinderance. In contrast, relatively smaller molecules of MB or AZB (diameter around 0.8 – 0.9 nm) showed slightly higher rate of IPD kinetics. We have observed that agarose gels release either MB or AZB a bit faster to blood smear in comparison to EY, indicating that both pore diffusion and the nature of interactions between charged molecules of thiazine and polysaccharide affect the apparently higher rate of desorption. However, this warrants further investigation with molecular spectroscopy including Fourier transform infrared spectroscopy (FT-IR), Raman spectroscopy and X-ray photoelectron spectroscopy (XPS) in conjunction with thermogravimetric analysis (TGA) [35].

The desorbed and adsorbed amount of Romanowski dyes to and from agarose gels is quantifiable in the time scale of RBC staining (desorption) and destaining (adsorption).

Despite the different time scale of experiments (**Figures 3** and **7**), we attempt to quantify the amount of each Romanowski dye transferred to and from agarose gels using the PSO kinetics model (**Table 2**) and the one phase decay model (**Table 3**). For example, the desorbed amount of the total of ternary mixture for 60 s estimated is 0.0430 nmole of EY, 0.533 nmole of MB and 0.853 nmole of AZB, which is presumably transferred to the smeared RBCs in the area of 3.2 cm^2. Data in **Table 4** and **Figures 7b, 7d** and **7f** show that the relative quantity of retained MB and AZB in agarose gels is higher indicating that blue staining is easier in earlier time points in comparison to red staining by agarose gels.

Table 4. Estimated amount of each dye per 14 mg agarose from the PSO kinetics model of adsorption and the one phase decay model of desorption, respectively.

Time (s)	Adsorption (nmole)			Desorption (nmole)		
	EY	**MB**	**AZB**	**EY**	**MB**	**AZB**
0	0.000	0.000	0.000	22.7	140	203
10	0.137	0.547	0.817	22.6	140	202
30	0.398	1.60	2.39	22.6	139	201
60	0.783	3.16	4.74	22.4	137	198

When using a mixture of these three Romanowski dyes in a single agarose gel for staining/destaining, the extent of staining/destaining can be adjusted by changing the ratio of each dye. However, since EY and AZB can precipitate when combined, there is a limitation to adjusting the ratio of stains. It may be more efficient to stain separately by combining appropriate Romanowski dyes with similar physical properties. Thus, staining with EY first may be useful due to its ability to stain blood cells relatively fast. Staining with MB or AZB later using another agarose gel can prevent discoloration due to higher amount of desorption (staining) (**Table 4**). However, it is important to stain MB and AZB for a sufficient time to prevent rapid adsorption (destaining) into the agarose gel and ensure discernible staining.

Changes of RBC colors by the solution-free hydrogel stamping occurs within 30 s and the assessment of such color changes is feasible with microscopy, as evidenced by **Figure 3**. In contrast, the measurement of concentrations with UV-Vis spectrometry in the same time scale is challenging due to relatively small changes within 60 s, as evidenced by the time scale of τ in **Table 3**. Another limitation is that three different dyes are measured at three different wavelengths to evaluate concentrations and their changes (**Figures S1** and **4**). Changes in adsorbed or desorbed dyes can be theoretically measured after dissolving agarose at higher temperature around 60°C while significant loss of samples and measurement errors are expected.

Application of the hydrogel stamps to blood films

As shown in **Figures 6** and **7**, the type of interaction of EY and MB/AZB are distinguished from the results of Langmuir isotherms and PSO kinetics. Thus, we separated EY and MB/AZB from the ternary mixture. This separation is always preferred due to the charged natures of Romanowsky dyes as well as the evaporation of methanol, which cause precipitation in solution. Therefore, separation of Romanowsky dyes in hydrogels can prevent unintended precipitation and the control of staining/destaining simply with contact time would be advantageous to quality control of RBC staining. Here, we demonstrate the quantitative assessment of stained/destained RBCs with three separate agarose gels by simply control the contact time between blood film and agarose gels.

In **Figure 8**, we varied the combination of three different agarose gels with contact time of 10 s, 30 s and 60 s. While 27 combinations (3 agarose gels and 3 different contact periods = 3^3) can be generated, we simplified the combination and extracted values of H with 9 combinations. With fixed staining of blue and clear agarose gels (**Figure 8a**), increasing the contact time of red agarose gel increased values of H (from mean values of 257 to 300). Corresponding images of RBC show the similar trend, showing increase of redness in the colors of RBC cytoplasm.

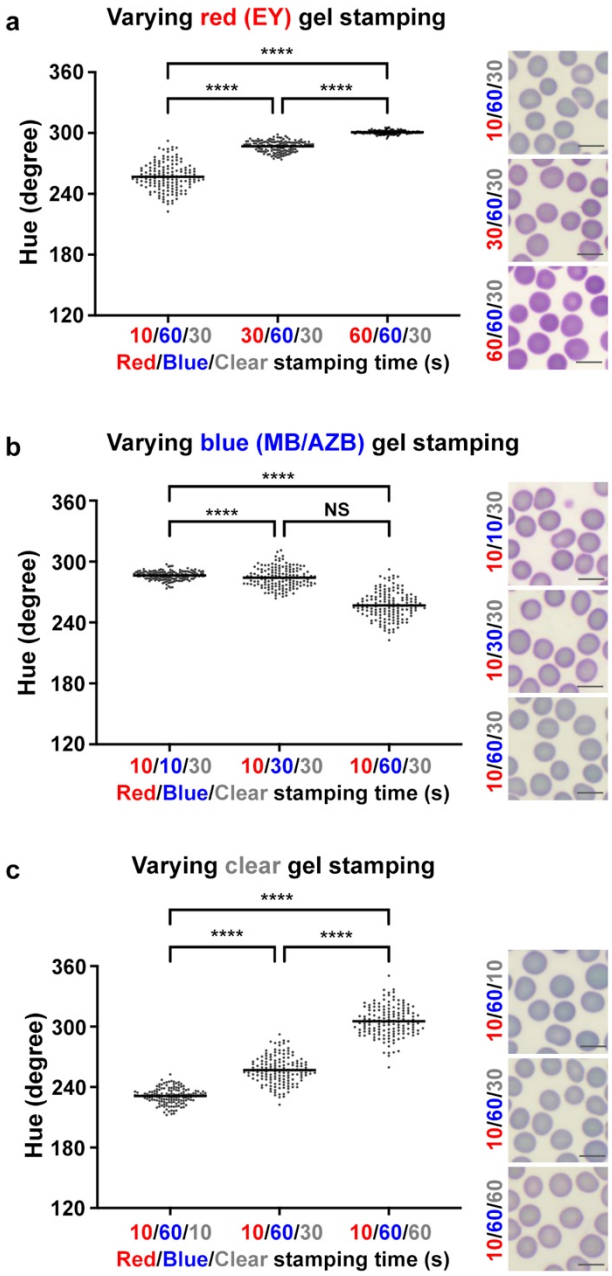

Figure 8. Application of the miLab^{TM} hydrogel stamps to RBC films. miLab agarose gels (red including EY, blue including MB/AZB and clear including no dyes) were applied to blood films at different combinations of staining and destaining time. H and representative images of stained and destained RBCs are reported with varying staining time of red (EY) (a), blue (MB/AZB) (b) and clear (c) agarose gels. One way ANOVA with Tukey's *post hoc* tests, ****p<0.0001 and NS (non-significant). Scatter dot plot with mean. Scale bar, 10 μm.

Similarly in **Figure 8b**, increasing the contact time of blue agarose gel decreased values of H (mean values of 286 to 257) and the blueness in RBC cytoplasm also increased. In **Figure 8c**, destaining with clear agarose gels increased values of H (from mean values of 231 to 305)

along with the changes of the corresponding colors in RBC cytoplasm. Background values of H are maintained relatively consistent as shown in **Figure S6** even though the contact time of agarose gel was increased. In comparison to values of S in **Figure S3**, those in **Figure S6** vary in a wider range from 0.07 to 0.23, which is primarily attributed to significantly higher concentrations of dyes in the miLab™ cartridge. As discussed above, the concentrations of the ternary mixture were much lower for analytical purposes: absorbance above 1.0 allows less than 10% of light to be transmitted through the sample (absorbance = $\log_{10}$ 100/% transmittance), which may sacrifice accuracy of absorbance measurements [36]. By separating EY and MB/AZB from the ternary mixture, it prevents the precipitation after forming the azure B-eosin complexes while providing larger possible formulation space for different combination of EY and MB/AZB concentrations.

Ironically, these important Romanowski dyes that are used to diagnose tissue and blood disorders are also water pollutants. Synthetic dyes in the form of water contaminants including MB and EY inhibit aquatic photosynthesis and expose humans and animals to the toxic food chains [37]. Unlike different strategies, adsorption could be viewed as a promising option for discharge of industrial and/or toxic dyes from wastewater because of its proficiency, high selectivity, minimal expense, simplicity of activity, effortlessness, and accessibility in a wide scope of trial conditions [38]. Thus, the hydrogel stamping technology potentially reduces the pollution to wastewater without sacrificing the performance of the Romanowsky staining.

Conclusions

We previously published the hydrogel stamping technology [4]. To better quantify the transferred amount of Romanowski dye molecules to and from agarose gels, we first tested if the transfer is quantifiable by measuring the extent of staining on smeared RBCs. Values of H gave us reasonable estimation, but precise quantification of the transfer needed a standard

curve method. Since Romanowski staining uses a ternary mixture and the sorption behavior of each dye is assumed to be different, we collected adsorption and desorption data to fit with predictable models. The ternary mixture shows predictable adsorption to agarose gels as evidenced by high goodness of fit with the Langmuir isotherms. We also found that the kinetics of adsorption is explained by the PSO kinetics model, where the nature of Romanowski dye is the determinant of the kinetics and that the kinetics of desorption shows exponential decay with a fraction of Romanowsky dye molecules retained in agarose gels due to the high affinity of Romanowsky dye molecules. Our methods applied in this study demonstrate that quantification of the transferred Romanowski dye molecules is feasible by bright filed microscopy with quantifying H values and UV-Vis spectrometry with established models of kinetics.

Conflict of interest statement

The authors declare the following competing financial interest(s): CYB, MJS, EH, SKB and YS are employees of Noul Co., Ltd. JPJ was a member of Scientific Advisory Board (Technical Consultant) in Noul Co., Ltd.

Author Contributions

JPJ and CYB conceived and designed the experiments. CYB, HE, MJS, EH, SKB and YS quantified sorption to and from agarose gels. SAZ measured viscoelasticity. BB analyzed the results of sorption experiments. JPJ, CYB and HE wrote the manuscript and all authors reviewed, edited and approved the manuscript.

Acknowledgements

This work was in part supported by the Korea Medical Device Development Fund grant funded by the Ministries of Science and ICT (Information and Communications Technology); Trade, Industry and Energy; Health and Welfare; Food and Drug Safety (Project Number:

1711174404, RS-2020-KD000092). The authors acknowledge the partial support from the Louisiana Board of Regents Research Competitiveness Subprogram (LEQSF(2018-21)-RD-A-03, JPJ), the National Science Foundation CAREER award (DMR-2047018, JPJ) and LSU Faculty Research Grant-Emerging Research (JPJ).

References

1. Correa, S., et al., *Translational Applications of Hydrogels.* Chemical Reviews, 2021. **121**(18): p. 11385-11457.
2. Cybulski, J.S., J. Clements, and M. Prakash, *Foldscope: origami-based paper microscope.* PloS one, 2014. **9**(6): p. e98781-e98781.
3. Kaur, T., et al., *Foldscope as a primary diagnostic tool for oral and urinary tract infections and its effectiveness in oral health education.* J Microsc, 2020. **279**(1): p. 39-51.
4. Choi, J.H., et al., *Hydrogel-Based Stamping Technology for Solution-Free Blood Cell Staining.* ACS Appl Mater Interfaces, 2021. **13**(19): p. 22124-22130.
5. Xiong, J.Y., et al., *Topology evolution and gelation mechanism of agarose gel.* J Phys Chem B, 2005. **109**(12): p. 5638-43.
6. Chen, Y., et al., *Environmentally Friendly Gelatin/β-Cyclodextrin Composite Fiber Adsorbents for the Efficient Removal of Dyes from Wastewater.* Molecules (Basel, Switzerland), 2018. **23**(10): p. 2473.
7. Erfani, M. and V. Javanbakht, *Methylene Blue removal from aqueous solution by a biocomposite synthesized from sodium alginate and wastes of oil extraction from almond peanut.* Int J Biol Macromol, 2018. **114**: p. 244-255.
8. Maruthapandi, M., et al., *Kinetics, Isotherm, and Thermodynamic Studies of Methylene Blue Adsorption on Polyaniline and Polypyrrole Macro-Nanoparticles Synthesized by C-Dot-Initiated Polymerization.* ACS Omega, 2018. **3**(7): p. 7196-7203.
9. Hayashi, A. and T. Kanzaki, *Swelling of agarose gel and its related changes.* Food Hydrocolloids, 1987. **1**(4): p. 317-325.
10. Fong Amaris, W.M., et al., *Image features for quality analysis of thick blood smears employed in malaria diagnosis.* Malar J, 2022. **21**(1): p. 74.
11. Fernández-Pérez, A. and G. Marbán, *Visible Light Spectroscopic Analysis of Methylene Blue in Water; What Comes after Dimer?* ACS Omega, 2020. **5**(46): p. 29801-29815.
12. Pospichal, R., et al., *Determination of chondroitin sulfate by thiazine dyes using flow injection analysis with spectrophotometric detection.* Analytical letters, 2007. **40**(6): p. 1167-1175.
13. Seow, W.Y. and C.A.E. Hauser, *Freeze–dried agarose gels: A cheap, simple and recyclable adsorbent for the purification of methylene blue from industrial wastewater.* Journal of Environmental Chemical Engineering, 2016. **4**(2): p. 1714-1721.
14. Abdullah, M., L. Chiang, and M. Nadeem, *Comparative evaluation of adsorption kinetics and isotherms of a natural product removal by Amberlite polymeric adsorbents.* Chemical Engineering Journal, 2009. **146**(3): p. 370-376.
15. Fairman, H.S., M.H. Brill, and H. Hemmendinger, *How the CIE 1931 color-matching functions were derived from Wright-Guild data.* Color Research & Application, 1997. **22**(1): p. 11-23.
16. Cruz, D., et al. *Determination of blood components (WBCs, RBCs, and Platelets) count in microscopic images using image processing and analysis*. in *2017IEEE 9th International Conference on Humanoid, Nanotechnology, Information Technology, Communication and Control, Environment and Management (HNICEM)*. 2017.
17. Yabusaki, K., et al., *A novel quantitative approach for eliminating sample-to-sample variation using a hue saturation value analysis program.* PLoS One, 2014. **9**(3): p. e89627.
18. Velastegui, R. and M. Pedersen. *The Impact of Using Different Color Spaces in Histological Image Classification using Convolutional Neural Networks*. in *2021 9th European Workshop on Visual Information Processing (EUVIP)*. 2021.

19. Bentley, S.A., P.N. Marshall, and F.E. Trobaugh, Jr., *Standardization of the Romanowsky staining procedure: an overview.* Anal Quant Cytol, 1980. **2**(1): p. 15-8.
20. Horobin, R.W., *How Romanowsky stains work and why they remain valuable - including a proposed universal Romanowsky staining mechanism and a rational troubleshooting scheme.* Biotech Histochem, 2011. **86**(1): p. 36-51.
21. Hajian, R. and A. Soltaninezhad, *The Spectrophotometric Multicomponent Analysis of a Ternary Mixture of Paracetamol, Aspirin, and Caffeine by the Double Divisor-Ratio Spectra Derivative Method.* Journal of Spectroscopy, 2013. **2013**: p. 405210.
22. Abdelwahab, N.S. and M.A. Mohamed, *Three New Methods for Resolving Ternary Mixture with Overlapping Spectra: Comparative Study.* Chem Pharm Bull (Tokyo), 2017. **65**(6): p. 558-565.
23. Janaky, N., X. Jun-Ying, and L. Xiang-Yang, *Determination of agarose gel pore size: Absorbance measurements vis a vis other techniques.* Journal of Physics: Conference Series, 2006. **28**(1): p. 83.
24. Golawska, S., et al., *Are agarose-sucrose gels useful for studying the probing and feeding behavior of aphids?* Australian Journal of Crop Science, 2014. **8**(2): p. 263.
25. Wang, S., et al., *The physical and surface chemical characteristics of activated carbons and the adsorption of methylene blue from wastewater.* J Colloid Interface Sci, 2005. **284**(2): p. 440-6.
26. Valdés, H., et al., *Effect of Ozone Treatment on Surface Properties of Activated Carbon.* Langmuir, 2002. **18**(6): p. 2111-2116.
27. Chakraborty, M. and A.K. Panda, *Spectral behaviour of eosin Y in different solvents and aqueous surfactant media.* Spectrochim Acta A Mol Biomol Spectrosc, 2011. **81**(1): p. 458-65.
28. Schulte, E., D. Wittekind, and V. Kretschmer, *The influence of cationic thiazine dyes on eosin Y-uptake of red blood cells in Romanowsky-Giemsa type stains.* Acta Histochem Suppl, 1989. **37**: p. 139-47.
29. Al-Ghouti, M.A. and R.S. Al-Absi, *Mechanistic understanding of the adsorption and thermodynamic aspects of cationic methylene blue dye onto cellulosic olive stones biomass from wastewater.* Sci Rep, 2020. **10**(1): p. 15928.
30. Hoseinzadeh Hesas, R., et al., *Preparation and Characterization of Activated Carbon from Apple Waste by Microwave-Assisted Phosphoric Acid Activation: Application in Methylene Blue Adsorption.* BioResources; Vol 8, No 2 (2013), 2013.
31. Sahoo, T.R. and B. Prelot, *Chapter 7 - Adsorption processes for the removal of contaminants from wastewater: the perspective role of nanomaterials and nanotechnology*, in *Nanomaterials for the Detection and Removal of Wastewater Pollutants*, B. Bonelli, et al., Editors. 2020, Elsevier. p. 161-222.
32. Xiao, Y., J. Azaiez, and J.M. Hill, *Erroneous Application of Pseudo-Second-Order Adsorption Kinetics Model: Ignored Assumptions and Spurious Correlations.* Industrial & Engineering Chemistry Research, 2018. **57**(7): p. 2705-2709.
33. Richter, A.P., et al., *An environmentally benign antimicrobial nanoparticle based on a silver-infused lignin core.* Nat Nanotechnol, 2015. **10**(9): p. 817-23.
34. Hubbe, M.A., S. Azizian, and S. Douven, *Implications of apparent pseudo-second-order adsorption kinetics onto cellulosic materials: A review.* BioResources, 2019. **14**(3): p. 7582-7626.
35. Yang, M., et al., *Preparation of κ-carrageenan/graphene oxide gel beads and their efficient adsorption for methylene blue.* J Colloid Interface Sci, 2017. **506**: p. 669-677.
36. Burke, R.W., E.R. Deardorff, and O. Menis, *Liquid Absorbance Standards.* J Res Natl Bur Stand A Phys Chem, 1972. **76a**(5): p. 469-482.

37. Yadav, S.K., S.R. Dhakate, and B. Pratap Singh, *Carbon nanotube incorporated eucalyptus derived activated carbon-based novel adsorbent for efficient removal of methylene blue and eosin yellow dyes.* Bioresour Technol, 2022. **344**(Pt B): p. 126231.
38. Katheresan, V., J. Kansedo, and S.Y. Lau, *Efficiency of various recent wastewater dye removal methods: A review.* Journal of environmental chemical engineering, 2018. **6**(4): p. 4676-4697.